

Scalar Glueball Mass Reduction at Finite Temperature in SU(3) Anisotropic Lattice QCD

Noriyoshi ISHII

The Institute of Physical and Chemical Research (RIKEN),
2-1 Hirosawa, Wako, Saitama 351-0198, JAPAN

Hideo SUGANUMA

Tokyo Institute of Technology,
2-12-1 Ohkayama, Meguro, Tokyo 152-8552, JAPAN

Hideo MATSUFURU

Yukawa Institute for Theoretical Physics, Kyoto University,
Kitashirakawa-Oiwake, Sakyo, Kyoto 606-8502, JAPAN

We report the first study of the glueball properties at finite temperatures below T_c using SU(3) anisotropic lattice QCD with $\beta = 6.25$, the renormalized anisotropy $a_s = a_t = 4$ and $20^3 N_t$ ($N_t = 35, 36, 37, 38, 40, 43, 45, 50, 72$) at the quenched level. From the temporal correlation analysis with the smearing method, about 20% mass reduction is observed for the lowest scalar glueball as $m_G(T) = 1.25 - 0.1 \text{ GeV}$ for $0.8T_c < T < T_c$ in comparison with $m_G \approx 1.5 - 1.7 \text{ GeV}$ at $T = 0$.

PACS numbers: 12.38.Gc, 12.39.Mk, 12.38.Mh, 11.15.Ha

Finite temperature QCD, including the quark gluon plasma (QGP) physics, is one of the most interesting subjects in the quark hadron physics [1, 2, 3]. At high temperature, in accordance with the asymptotic freedom of QCD, the strong interaction among quarks and gluons is expected to be reduced, and there would occur the deconfinement and/or chiral phase transition [1].

For the study of finite temperature QCD, the lattice QCD Monte Carlo simulation provides a reliable method directly based on QCD. For instance, SU(3) lattice QCD simulations at the quenched level show a weak first-order deconfinement phase transition at the critical temperature $T_c \approx 260 \text{ MeV}$ [4], and full SU(3) QCD simulations show a chiral phase transition at $T_c = 173(8) \text{ MeV}$ for $N_f = 2$ and $154(8) \text{ MeV}$ for $N_f = 3$ in the chiral limit [5]. Above T_c , most of the nonperturbative properties such as color confinement and spontaneous chiral-symmetry breaking disappear, and quarks and gluons are liberated.

Even below T_c , there are many model predictions on the change of the hadron properties [2, 6, 7], the mass and the size, due to the change in the inter-quark potential [8, 9] and the partial chiral restoration. Nevertheless, lattice QCD studies for thermal properties of hadrons are still inadequate at present because of the difficulty in measuring the hadronic two-point correlators on the lattice at finite temperature. For instance, on the screening mass measurement [10], this difficulty is due to the mixture of the large Matsubara frequencies in addition to the absence of technical prescriptions as the smearing method. On the other hand, on the pole-mass measurement, while it is free from the mixture of the Matsubara frequencies, another difficulty arises from the shrink of the physical temporal size $l=T$ at high temperature. In fact, the pole-mass measurements have to be performed within the limited distance shorter than $l=(2T)$, and such

a limitation corresponds to $N_t = 4 - 8$ near T_c in the ordinary isotropic lattice QCD [4].

To avoid this severe limitation on the temporal size, we adopt an anisotropic lattice where the temporal lattice spacing a_t is smaller than the spatial one a_s [8, 11, 12, 13]. We can thus efficiently use a large number of the temporal lattice points as $N_t \approx 32$ even near T_c , while the physical temporal size is kept fixed $l=T = N_t a_t$. In this way, the number of available temporal data is largely increased, and accurate pole-mass measurements from the temporal correlation become possible [12, 13].

In this paper, we study the glueball at finite temperature from the temporal correlation analysis, using SU(3) anisotropic lattice QCD at the quenched level, where dynamical quarks are absent. Even without dynamical quarks, QCD still possesses a lot of important nonperturbative features such as color confinement, the instanton effects and the non-vanishing gluon condensate. Unlike full QCD, the elementary excitations are only glueballs in the confinement phase below $T_c \approx 260 \text{ MeV}$. At zero temperature, the lightest physical excitation is a scalar glueball with $J^{PC} = 0^{++}$ with the mass $m_G \approx 1.5 - 1.7 \text{ GeV}$ [13, 14, 15, 16], which is expected to dominate the thermodynamical properties below T_c .

We consider the glueball correlator [13, 14, 15, 16, 17, 18] in SU(3) lattice QCD_X as $G(t) = \langle h^\dagger(t) \sigma(0) i, \sigma(t) = \langle O(t) = \langle h^\dagger i, O(t) = \langle O(t; \mathbf{x}) \rangle$. The summation over \mathbf{x} physically means the zero-momentum projection. The glueball operator $O(t; \mathbf{x})$ is to be properly taken so as to reproduce its quantum number J^{PC} in the continuum limit. For instance, the simplest composition for the scalar glueball is given as $O(t; \mathbf{x}) = \text{ReTr} P_{12}(t; \mathbf{x}) + P_{23}(t; \mathbf{x}) + P_{31}(t; \mathbf{x}) g$, where $P(t; \mathbf{x})$ is the SU(3) plaquette operator. With the spec-

tral representation, $G(t)$ is expressed as $G(t) = G(0) = \sum_n c_n e^{-E_n t}$, $c_n = \int \mathcal{D}i \mathcal{D}j \mathcal{D}i j^2 = G(0)$, $G(0) = \int \mathcal{D}i \mathcal{D}j \mathcal{D}i j^2$, where E_n denotes the energy of the n -th excited state $|j_i\rangle$. Here, $|i\rangle$ denotes the vacuum, and $|j_i\rangle$ denotes the ground-state glueball. Note that c_n is a non-negative number with $c_0 = 1$. On a fine lattice with the spacing a , the simple plaquette operator $P_{ij}(t; \mathbf{x})$ has a small overlap with the glueball ground state $|j_i\rangle$, and the extracted mass looks heavier owing to the excited-state contamination. This small overlap problem originates from the fact that $O(t; \mathbf{x})$ has a smaller "size" of $O(a)$ than the physical peculiar size of the glueball. This problem becomes severer as $a \rightarrow 0$. We thus have to improve $O(t; \mathbf{x})$ so as to have almost the same size as the physical size of the glueball.

One of the systematic ways to achieve this is the smearing method [18, 19, 20]. The smearing method is expressed as the iterative replacement of the original spatial link variables $U_i(s)$ by the associated fat link variables, $\bar{U}_i(s)$ 2 SU(3) $_c$, which is defined so as to maximize

$$\text{ReTr} \bar{U}_i^y(s) = U_i(s) + \sum_{j \in \hat{i}} U_j(s) U_i(s \hat{j}) U_j^y(s + \hat{i}) ; \quad (1)$$

where $U_i(s) = U^y(s \hat{i})$, and \hat{i} is a real parameter. Here, the summation is taken only over the spatial direction to avoid the nonlocal temporal extension. Note that $\bar{U}_i(s)$ holds the same gauge transformation properties with $U_i(s)$. We refer to the fat link defined in Eq. (1) as the first fat link $U_i^{(1)}(s)$. The n -th fat link $U_i^{(n)}(s)$ is defined iteratively as $U_i^{(n)}(s) = \bar{U}_i^{(n-1)}(s)$ starting from $U_i^{(1)} = \bar{U}_i(s)$ [20]. For the physically extended glueball operator, we use the n -th smeared operator, the plaquette operator constructed with $\bar{U}_i^{(n)}(s)$.

Next, we consider the size of the n -th smeared operator. Using the linearization and the continuum approximation, we obtain the diffusion equation as [13, 21]

$$\frac{\partial}{\partial n} \ln \langle i(n; \mathbf{x}) \rangle = D \Delta \ln \langle i(n; \mathbf{x}) \rangle; \quad D = \frac{a_s^2}{4}; \quad (2)$$

where a_s denotes the spatial lattice spacing. $\ln \langle i(n; \mathbf{x}) \rangle$ describes the distribution of the gluon field $A_i(\mathbf{x}; t)$ in the n -th smeared plaquette. The n -th smeared plaquette located at the origin $\mathbf{x} = \mathbf{0}$ physically means the Gaussian extended operator with the distribution as [13, 21]

$$\ln \langle i(n; \mathbf{x}) \rangle = \frac{1}{(4 - Dn)^{3=2}} \exp \left(-\frac{\mathbf{x}^2}{4Dn} \right); \quad (3)$$

Hence the size of the operator is estimated as

$$R \sim \sqrt{\frac{6n}{4D}} = \sqrt{\frac{6n}{4 \cdot \frac{a_s^2}{4}}} = a_s \sqrt{\frac{6n}{4}}; \quad (4)$$

So far, the smearing method is introduced to carry out the accurate mass measurement by maximizing the

ground-state overlap. However, it can be also used to give a rough estimate of the physical glueball size. In fact, once we obtain the maximum overlap with some n and a , the glueball size is estimated with Eq. (4).

We use the SU(3) anisotropic lattice plaquette action

$$S_G = \frac{1}{N_c} \sum_{s; i < j} \text{ReTr} (1 - P_{ij}(s)) + \frac{1}{N_c} \sum_{s; i} \text{ReTr} (1 - P_{i4}(s)) \quad (5)$$

with the plaquette operator $P_{ij}(s)$ 2 SU(3) in the (i, j) -plane. The lattice parameter is fixed as $2N_c = g^2 = 6.25$, and the bare anisotropy parameter is taken as $\beta_0 = 3.2552$ so as to reproduce the renormalized anisotropy $a_s = a_t = 4$ [11]. These parameters produce the spatial lattice spacing as $a_s^{-1} = 2.272(16)$ GeV ($a_s \approx 0.087$ fm), and the temporal one as $a_t^{-1} = 9.088(64)$ GeV ($a_t \approx 0.022$ fm). Here, the scale unit is determined by adjusting the string tension as $\sigma = 427$ MeV from the on-axis data of the static inter-quark potential. The pseudo-heat-bath algorithm is used to update the gauge field configurations on the lattice of the sizes $20 \times N_t \times N_t$ = 35, 36, 37, 38, 40, 43, 45, 50, 72. The corresponding temperatures are listed in Table I. For each temperature, we pick up gauge field configurations every 100 sweeps for measurements, after skipping more than 20,000 sweeps of the thermalization. The numbers of gauge configurations used in our calculations are summarized in Table I.

From the analysis of the Polyakov loop $\langle P(\mathbf{x}) \rangle = \langle \text{Tr} U_4(\mathbf{x}; 0) \rangle = \langle \text{Tr} U_4(\mathbf{x}; N_t) \rangle$, we obtain $T_c \approx 260$ MeV, which is consistent with the previous studies [4, 8].

We present the numerical results in SU(3) anisotropic lattice QCD at the quenched level. To enhance the ground-state contribution, we adopt the smearing method with the smearing parameter $\beta = 2.1$, which we find one of the most suitable values from the numerical tests with various β . The statistical errors are estimated with the jackknife analysis [17].

In Fig. 1, we show a scalar glueball correlator $G(t) = G(0)$ at a low temperature $T = 125$ MeV for $N_{\text{smeared}} = 40$, where all the lattice QCD data with $1 \leq t \leq 24$ are well fitted by a single hyperbolic cosine, denoted by the solid curve, as

$$G(t) = G(0) = C (e^{-m_G t a_t} + e^{-m_G (N_t - t) a_t}); \quad (6)$$

This indicates the achievement of the ground-state enhancement owing to the smearing method, and then the excited-state contamination is almost removed.

In general, $G(t) = G(0)$ is expressed as a weighted sum of hyperbolic cosines with non-negative weights, and $G(t) = G(0)$ decreases more rapidly than Eq. (6) near $t = 0$ due to excited-state contributions. Hence, C should satisfy the inequality $C \leq (1 + e^{-m_G a_t N_t})^{-1} \approx 1$. In the ground-state dominant case, $G(t) = G(0)$ can be well approximated by a single hyperbolic cosine, and $C \approx 1$ is realized. We refer to C as the ground-state overlap.

TABLE I: The lattice QCD result for the lowest scalar glueball mass at finite temperature. The temporal lattice points N_t , the corresponding temperature T , the lowest scalar glueball mass $m_G(T)$, the maximal value of the ground-state overlap C^{\max} , uncorrelated χ^2/N_{DF} , the smearing number $N_{\text{smear}}^{\text{best}}$, the smearing window $N_{\text{smear}}^{\text{window}}$ and the glueball size $R' \approx \sqrt{2} \ln^2 2$ are listed. The most suitable smearing number $N_{\text{smear}}^{\text{best}}$ is determined with the maximum ground-state overlap condition.

N_t	T [MeV]	m_G [GeV]	C^{\max}	χ^2/N_{DF}	$N_{\text{smear}}^{\text{best}}$	$N_{\text{smear}}^{\text{window}}$	$N_{\text{con g}}$	R [fm]
72	125	1.54(1)	0.981(6)	0.23	41	32 51	1284	0.49 0.61
50	182	1.43(2)	0.967(8)	0.02	45	36 55	1051	0.52 0.64
45	202	1.48(2)	0.971(8)	0.08	37	30 46	1382	0.47 0.58
43	210	1.30(2)	0.945(8)	0.35	40	32 52	1197	0.49 0.62
40	227	1.29(2)	0.935(6)	1.22	40	32 51	2021	0.49 0.61
38	239	1.36(2)	0.935(7)	1.00	38	30 50	2030	0.47 0.61
37	245	1.18(3)	0.889(12)	0.91	43	35 53	2150	0.51 0.63
36	252	1.38(2)	0.948(8)	0.09	36	29 46	1744	0.46 0.58
35	259	1.26(2)	0.931(7)	1.15	40	31 51	2244	0.48 0.61

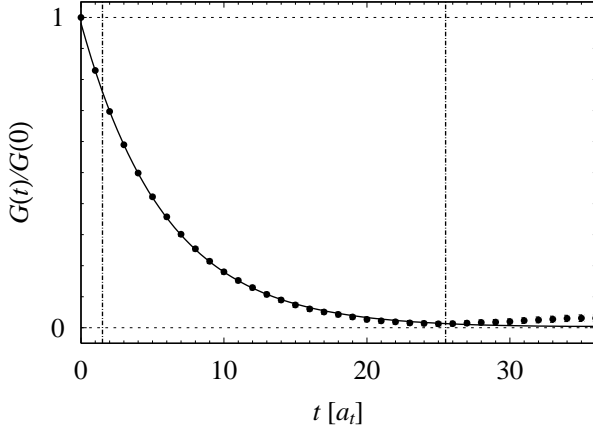


FIG. 1: The scalar glueball correlator $G(t)=G(0)$ plotted against t for $N_{\text{smear}} = 40$ at a low temperature $T = 125$ MeV. The statistical errors with the jackknife analysis are hidden within the symbol. The solid curve denotes the best single hyperbolic cosine fit to the lattice data in the interval indicated by the two vertical dashed lines.

From Fig. 1, we find $C' \approx 1$ and $m_G \approx 1.54$ GeV for the lowest scalar glueball mass at a low temperature. This seems consistent with $m_G \approx 1.5 - 1.7$ GeV at $T = 0$ [14, 15, 16].

In Fig. 2, we show a scalar glueball correlator $G(t)=G(0)$ at a high temperature $T = 245$ MeV for $N_{\text{smear}} = 40$. Owing to a suitable smearing, the lattice QCD data with $3 \leq t \leq 17$ are well fitted by a single hyperbolic cosine denoted by the solid curve.

We perform the best fit analysis in the interval $[t_{\text{min}}; t_{\text{max}}]$, which is determined from the flat region $[t_{\text{min}}; t_{\text{max}} - 1]$ appeared in the corresponding "effective mass" plot. The effective mass $m_e(t)$ is a solution of

$$\frac{G(t+1)}{G(t)} = \frac{\cosh(m_e(t)a_t(t+1 - N_t=2))}{\cosh(m_e(t)a_t(t - N_t=2))}; \quad (7)$$

for a given $G(t+1)=G(t)$ at each fixed t [17].

In the most suitable smearing $N_{\text{smear}}^{\text{best}}$, the ground-state

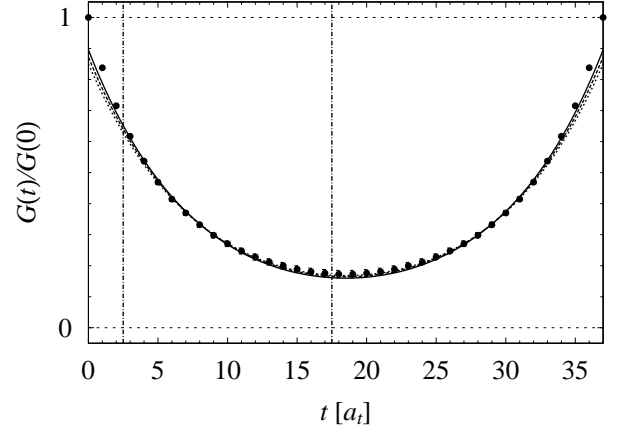


FIG. 2: The scalar glueball correlator $G(t)=G(0)$ plotted against t for $N_{\text{smear}} = 40$ at a high temperature $T = 245$ MeV. The statistical errors are hidden within the symbol. The solid curve denotes the best single hyperbolic cosine fit to the lattice data in the interval $[t_{\text{min}}; t_{\text{max}}]$ indicated by the two vertical dashed lines. The dashed and dotted curves are the best hyperbolic cosine curves for the modified t range with $t_{\text{min}} + 1$ and $t_{\text{min}} + 2$, respectively. The closeness of the three curves means small t -range dependence.

overlap C is maximized and the mass m_G is minimized, which indicates the achievement of the ground-state enhancement. (For extremely large N_{smear} , the operator size exceeds the physical glueball size, resulting in the decrease of the overlap C .) In practical calculations, the maximum overlap and the mass minimization are achieved at almost the same N_{smear} , and both of these two conditions would work as an indication of the maximal ground-state enhancement. Here, we take the maximal ground-state overlap condition as $C' \approx 1$. (The mass minimization condition leads to almost the same glueball mass [21].)

From the analysis at various temperatures, we plot the lattice QCD result for the lowest scalar glueball mass $m_G(T)$ (solid circle) against temperature T in Fig. 3 to-

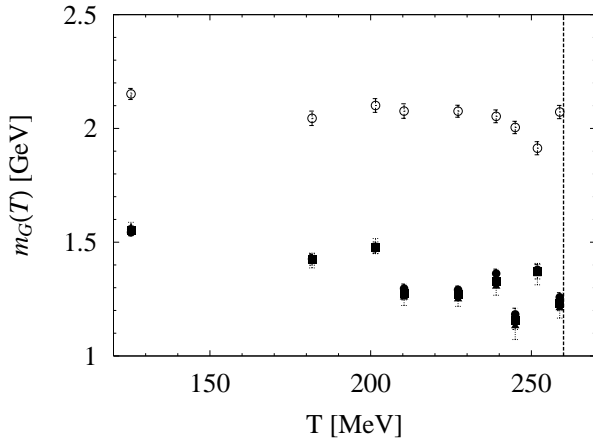


FIG. 3: The lowest scalar glueball mass (solid circle, square, triangle) and the 2^{++} glueball mass (open circle) plotted against the temperature T . They are obtained with the best hyperbolic cosine fit in the interval $[t_{\min}; t_{\max}]$ determined from the flat region in the effective mass plot. The solid square and triangle denote the scalar glueball masses obtained with the modified range with $t_{\min} + 1$ and $t_{\min} + 2$, respectively. The vertical dotted line indicates $T_c \approx 260$ MeV.

gether with the 2^{++} tensor glueball mass (open circle). We observe, in Fig. 3, about 20% mass reduction or a few hundred MeV mass reduction of the lowest scalar glueball near T_c as $m_G(T) = 1.25 \pm 0.1$ GeV for $0.8T_c < T < T_c$ in comparison with $m_G(T=0) \approx 1.5 \pm 0.1$ GeV [14, 15, 16]. The 2^{++} glueball mass seems almost unchanged.

To estimate the glueball size, we search $N_{\text{sm ear}}^{\text{best}}$ and C^{max} which realize the overlap maximum condition. Considering about 0.5% errors of C , we define the "smearing window" of $N_{\text{sm ear}}^{\text{window}}$ where $C \approx 0.995 C^{\text{max}}$ is satisfied. From Eq. (4) with $N_{\text{sm ear}}^{\text{window}}$, we estimate the glueball size as $R \approx 0.5 \pm 0.6$ fm both at low temperature and at high temperature near T_c .

In Table I, we summarize the lowest scalar glueball

mass $m_G(T)$, the ground-state overlap C^{max} , uncorrelated $^2=N_{\text{DF}}, N_{\text{sm ear}}^{\text{best}}, N_{\text{sm ear}}^{\text{window}}$, the number of gauge configurations $N_{\text{con g}}$ and the glueball size R .

Several comments are in order.

(i) The choice of the t range $[t_{\min}; t_{\max}]$ provides a possible source of the systematic error. To estimate this type of the systematic error, we perform further two fits in the modified two intervals, $[t_{\min} + 1; t_{\max}]$ and $[t_{\min} + 2; t_{\max}]$. Note that results are less sensitive to the choice of t_{\max} than t_{\min} , since the error bar of $G(t)=G(0)$ is larger for larger t . In Fig. 2, we also show the results of these two fits by dashed line and dotted line, respectively. The closeness of the three curves suggests small t -range dependence. In Fig. 3, the scalar glueball masses obtained with these two fits are added by solid square and solid triangle, respectively. The t -range dependence is found to be rather small.

(ii) In this paper, we mainly use the glueball operator composed of the smeared plaquettes, i.e., the smeared 1×1 loops. We analyze also the glueball properties using the glueball operators composed of the smeared loops with the size $N \times N$ ($N = 1; 2; \dots; 8$), and find almost the same results for the glueball mass.

(iii) The present results seem consistent with our previous work [13], where we used the $O(a^2)$ -improved anisotropic lattice action at $T = 0.87T_c$, and found a slight mass reduction of the lowest scalar glueball.

To summarize, we have studied the glueball properties at finite temperature using SU(3) anisotropic quenched lattice QCD with more than 1,000 gauge configurations at each temperature. From the temporal correlation analysis with the smearing method, we have observed about 20% mass reduction of the lowest scalar glueball as $m_G(T) = 1.25 \pm 0.1$ GeV for $0.8T_c < T < T_c$, while no significant change is seen for meson masses near T_c [12].

H. S. is supported by Grant for Scientific Research (No.12640274) from the Ministry of Education, Culture, Science and Technology, Japan. The lattice calculations have been performed on NEC-SX5 at Osaka University.

[1] W. Greiner and A. Schafer, "Quantum Chromodynamics", (Springer-Verlag, Berlin, 1994) 1.
[2] T. Hashimoto, K. Hirose, T. Kanki and O. Miyamura, Phys. Rev. Lett. 57 (1986) 2123.
[3] T. Matsui and H. Satz, Phys. Lett. B 178 (1986) 416.
[4] G. Boyd, J. Engels, F. Karsch, E. Laermann, C. Legeland, M. Lutgemeier, B. Petersson, Nucl. Phys. B 469 (1996) 419.
[5] F. Karsch, E. Laermann and A. Peikert, Nucl. Phys. B 605 (2001) 579.
[6] T. Hatsuda and T. Kunihiro, Phys. Rev. Lett. 55 (1985) 158.
[7] H. Ichie, H. Suganuma, H. Toki, Phys. Rev. D 52 (1995) 2944.
[8] H. Matsuñiru et al., Proc. of Quantum Chromodynamics and Color Confinement, edited by H. Suganuma et al. (World Scientific, 2001) 246.
[9] O. Kaczmarek, F. Karsch, E. Laermann and M. Lutgemeier, Phys. Rev. D 62 (2000) 034021.

[10] C. DeTar and J. B. Kogut, Phys. Rev. Lett. 59 (1987) 399.
[11] T. R. Klassen, Nucl. Phys. B 533 (1998) 557.
[12] QCD-Taro Collaboration, Phys. Rev. D 63 (2001) 054501.
[13] N. Ishii, H. Suganuma and H. Matsuñiru, Proc. of Lepton Scattering, Hadrons and QCD, (World Scientific, 2001).
[14] C. J. Morningstar and M. Peardon, Phys. Rev. D 60 (1999) 034509, and references therein.
[15] J. Sexton, A. Vaccarino and D. Weingarten, Phys. Rev. Lett. 75 (1995) 4563, and references therein.
[16] M. J. Teper, OUP-98-88-P (1998), hep-th/9812187.
[17] I. Montvay and G. Münster, Quantum Fields on a Lattice, (Cambridge, 1994) 1.
[18] H. J. Rothe, Lattice Gauge Theories, (World Scientific, 1992) 1.
[19] APE Collaboration, Phys. Lett. B 192 (1987) 163.
[20] T. T. Takahashi, H. Matsuñiru, Y. Nemoto and H. Sug-

anum a, Phys. Rev. Lett. 86 (2001) 18.

[21] N. Ishii, H. Suganuma and H. Matsufuru, in preparation.